

## Synthesis of Fentanyl Triazole Derivatives and their Affinity for Mu-Opioid and Sigma-1 Receptors

Ruth P. Paulino,<sup>a</sup> Rosemeire B. Alves,<sup>a</sup> Joanna Matalińska,<sup>b</sup> Piotr F. J. Lipiński<sup>b</sup> and Rossimiriam P. Freitas<sup>ib</sup>\*,<sup>a</sup>

<sup>a</sup>Departamento de Química, ICEx, Universidade Federal de Minas Gerais, Av. Pres. Antônio Carlos 6627 Pampulha, 31270-901 Belo Horizonte-MG, Brazil

<sup>b</sup>Department of Neuropeptides, Mossakowski Medical Research Institute Polish Academy of Sciences, 5 Pawińskiego Street, PL 02-106, Warsaw, Poland

The search for compounds with affinity for both mu-opioid receptor (MOR) and sigma-1 receptor ( $\sigma$ 1R) is one of the innovative directions to develop painkillers with reduced side effects. Additionally, triazole scaffolds have been extensively explored in the last two decades in medicinal chemistry. In this context, we synthesized a series of new triazole fentanyl derivatives and evaluated their affinity for both MOR and  $\sigma$ 1R. The binding affinity of the compounds for human MOR was determined in competitive radioligand binding assays, using fentanyl as standard. For the assays with  $\sigma$ 1R, a  $\sigma$ 1R agonist (SKF10047) was employed. The most active analogue was **6d** which moderately binds to MOR with half-maximal inhibitory concentrations ( $IC_{50}$ ) = 1.9  $\mu$ M and to  $\sigma$ 1R with  $IC_{50}$  = 6.9  $\mu$ M. Molecular docking calculations were carried out, providing a structural elucidation for the observed values of affinity. Absorption, distribution, metabolism, and excretion toxicity (ADMET) parameters for the new compounds were simulated with the SwissADME tool.

**Keywords:** opioids, MOR, sigma-1 receptor, fentanyl, triazole ring

### Introduction

Opioids, especially mu-opioid receptor (MOR) agonists, represent a class of compounds that have been used clinically for a long time, especially in the treatment of moderate to severe pain.<sup>1</sup> Thus, these drugs are prescribed for a wide range of indications, such as postoperative, inflammatory, trauma-related, and metastatic cancer pain.<sup>2,3</sup> Among the most employed opioids nowadays, morphine, oxycodone, hydrocodone, methadone, and fentanyl stand out.<sup>4</sup> Nonetheless, their use may lead to critical adverse side effects such as potential respiratory arrest, development of tolerance, addiction, drowsiness, and constipation. Moreover, the abuse of opioids, especially in North America, displays concerns for public authorities given the high number of deaths by overdose and it is estimated that 1-2 million people could die from it by 2029.<sup>5</sup>

Fentanyl is a synthetic opioid from the family of 4-anilidopiperidines first synthesized by Paul Janssen

in 1960 and is a very strong MOR agonist, largely used in medicine as an anesthetic.<sup>6</sup> Its high lipophilia makes fentanyl 50-100 times more potent than morphine and provides a fast onset of action.<sup>6</sup> However, it is also used as a drug of abuse with other opioids, like heroin, because it enhances the sensation of euphoria and analgesia. Consequently, fentanyl has been widely studied and a large number of derivatives have been synthesized to model its pharmacodynamic properties and understand its structure-activity relationships (SAR).<sup>7-9</sup> The most relevant properties related to SAR studies are shown in Figure 1. The key observations from SAR studies of fentanyl are: (i) the six-membered piperidine ring (region A) in chair conformation is ideal for the interaction of the opioid with the MOR, since the change of the ring to a pyrrolidine (5-membered) or azepane (7-membered) ring causes significant loss of analgesia; (ii) increasing or decreasing the length of the ethylene chain connecting the piperidine ring to the benzene ring (region B) reduces the analgesic effects of fentanyl and its derivatives; (iii) the benzyl rings, attached to the ethylene group (region B) or in the anilido moiety (region C) of fentanyl, are involved

\*e-mail: rossipfreitas@gmail.com

Editor handled this article: Brenno A. D. Neto

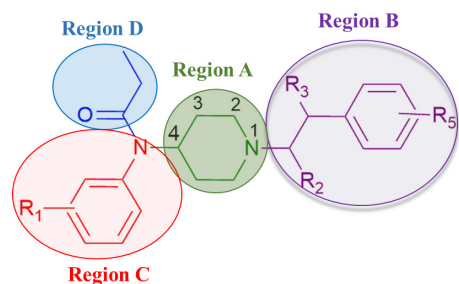


**Figure 1.** Structure of fentanyl and its disassembly reported by regions.

in lipophilic interactions of the compound with the MOR; (iv) the propionyl group (region D) has a relevant role in interactions with the MOR, and is related with electronic interactions with the receptor.

The sigma-1 receptor ( $\sigma$ 1R) is a one-of-a-kind chaperone protein, which was discovered in 1976 by Gilbert and Martin<sup>10</sup> and then was wrongly mistaken for an opioid receptor.<sup>10,11</sup> Since its discovery, several papers<sup>12-15</sup> have been written to exploit the role of  $\sigma$ 1R on psychological effects such as addiction, pain, depression, schizophrenia, strokes, and others. Another crucial point about  $\sigma$ 1R is its affinity for many ligands with high structural diversity such as butyrophenones, phenothiazines, thioxanthenes, anxiolytics, tricyclic antidepressants, 4-*N*-piperidines and also drugs of abuse such as cocaine, methamphetamine, and 3,4-methylenedioxymethamphetamine (MDMA).<sup>16,17</sup> Those studies have highlighted the importance of  $\sigma$ 1R as a biological target in the search for new ligands relevant to many areas of the medicinal field.<sup>18</sup> However, even though several molecules are under clinical trials for the treatment of neurodegenerative diseases, mental disorders, and pain management, no selective ligand has been approved for medicinal use thus far.<sup>19-21</sup> Since the relationship between the  $\sigma$ 1R and the MOR was established in the literature, the proposal of new ligands with bifunctional MOR agonists and  $\sigma$ 1R antagonists is urgently needed for therapeutical purposes, aiming the capacity of pain relief with reduced side effects.<sup>22,23</sup>

Although many fentanyl derivatives have been synthesized in the last decades in the search for an improved drug, only recently the preparation of fentanyl triazole derivatives was described in the literature.<sup>24</sup> The 1,2,3-triazoles display a broad range of pharmacological properties and can be easily prepared by click chemistry, in a copper(I)-catalyzed alkyne-azide cycloaddition (CuAAC) reaction.<sup>25</sup> In our ongoing efforts to identify hit molecules containing triazole compounds with biological activity, the present study brings the synthesis of novel fentanyl triazole derivatives and the evaluation of their affinity for the receptors  $\sigma$ 1R and MOR, in a hitherto unprecedented approach.

## Experimental

### Instruments and chemicals

Reagents were obtained from Vetec (Rio de Janeiro, Rio de Janeiro, Brazil), Sigma-Aldrich (St. Louis, Missouri, United States), Synth (Diadema, São Paulo, Brazil) and Oakwood Chemical (Estill, South Carolina, United States) and used without further purification. The solvents were purchased from Sigma-Aldrich (St. Louis, Missouri, United States), Vetec (Rio de Janeiro, Rio de Janeiro, Brazil), and Synth (Diadema, São Paulo, Brazil) and were distilled before use. The chemical reactions were monitored by thin layer chromatography (TLC), using aluminum-backed 60 F254 silica plates from Merck (Darmstadt, Hessen, Germany), under UV light at 254 nm. For the purification of the reaction products, column chromatography (CC) was performed using silica gel SiliCycle (Quebec City, Quebec, Canada) (0.035-0.070 mm, pore diameter 6 nm). Melting points were determined on MQAPF-302 apparatus from Microquimica (Palhoça, Santa Catarina, Brazil) melting point apparatus and are uncorrected. The nuclear magnetic resonance (NMR) spectra were recorded on a Bruker (Billerica, Massachusetts, United States) Nanobay 400 MHz using deuterated chloroform ( $\text{CDCl}_3$ ) from Sigma-Aldrich (São Paulo, São Paulo, Brazil) with tetramethylsilane (TMS) as an internal standard or the appropriate residual solvent peak. The respective chemical shifts ( $\delta$ ) were expressed in parts *per million* (ppm) and the coupling constant ( $J$ ) in hertz. Peaks are described as singlets (s), doublets (d), doublet of doublets (dd), triplets (t), quartets (q), septets and multiplets (m). High resolution mass spectra (HRMS) were obtained by electron spray ionization-mass spectrometry (ESI-MS) technique on a Q-Exactive from a Thermo Scientific (Waltham, Massachusetts, United States) mass spectrometer and Solarix from a Bruker (Bremen, Bremen, Germany) mass spectrometer.

### General procedures for the synthesis of 1-(2-azidoethyl) piperidin-4-one (**2**)

To a sealed tube containing a stirred solution of sodium azide (0.117 g, 1.8 mmol) in acetone (3 mL) was added 1,2-dibromoethane (**1**) (0.25 mL, 2.9 mmol). The resulting mixture (mixture 1) was maintained at room temperature for 24 h under magnetic stirring. In a different flask, 4-piperidone monohydrate hydrochloride was dissolved in 10 mL of acetone and the solution was treated with sodium carbonate ( $\text{K}_2\text{CO}_3$ ) (1.09 g, 7.92 mmol) and stirred at room temperature for 1 h (mixture 2). After this time,

mixture 1 was slowly added to mixture 2 and the resulting suspension was stirred and refluxed for 18 h. The reaction mixture was cooled to room temperature and extracted with dichloromethane ( $\text{CH}_2\text{Cl}_2$ ) ( $3 \times 15$  mL) and  $\text{H}_2\text{O}$  (10 mL). The organic layers were combined and washed with saturated solution of sodium bicarbonate ( $\text{NaHCO}_3$ ) ( $2 \times 10$  mL), dried over with sodium sulfate ( $\text{Na}_2\text{SO}_4$ ) and concentrated under reduced pressure to provide a yellow oil. The crude compound was purified by column chromatography using gradient elution of 0-20% of ethyl acetate in hexane ( $v v^{-1}$ ) to provide **2** as a light-yellow oil with 40% yield (120 mg, 0.71 mmol).  $^1\text{H}$  NMR (400 MHz,  $\text{CDCl}_3$ )  $\delta$  3.39 (t,  $J$  6.0, 2H), 2.84 (t,  $J$  6.0, 4H), 2.74 (t,  $J$  6.0, 2H), 2.49 (t,  $J$  6.0, 4H);  $^{13}\text{C}$  NMR (100 MHz,  $\text{CDCl}_3$ )  $\delta$  208.6, 56.3, 53.2 (2C), 48.7, 41.2 (2C); HRMS (ESI)  $m/z$ , calcd. for  $\text{C}_{12}\text{H}_{12}\text{N}_4\text{O}$  [ $\text{M} + \text{H}$ ] $^+$ : 169.10447, found: 169.10797.

#### General procedures for the synthesis of triazoles **4a-4e**

In a round bottom flask, it was added compound **2** (1.0 equiv.) dissolved in 5 mL of  $\text{CH}_2\text{Cl}_2$  followed by the addition of the corresponding alkyne (**3a-3e**) (phenylacetylene, *tert*-butyl prop-2-yn-1-yl-carbamate, 1-methoxy-3-(prop-2-yn-1-yloxy)benzene, 1-(prop-2-yn-1-yloxy)naphthalene and 4-pentyn-1-ol) (1.0 equiv.),  $\text{CuSO}_4 \cdot 5\text{H}_2\text{O}$  (0.2 equiv.), sodium ascorbate (0.4 equiv.) and 2 mL of  $\text{H}_2\text{O}$ . The reaction mixture was stirred at room temperature for 24 h. After completion of the reaction, 10 mL of water was added to mixture, followed by extraction with  $\text{CH}_2\text{Cl}_2$  ( $3 \times 15$  mL). The organic layers were combined and washed three times with a 25% ethylenediaminetetraacetic acid (EDTA) solution buffered with ammonium chloride ( $\text{NH}_4\text{Cl}$ ) at pH 9.5. The organic layer was dried with  $\text{Na}_2\text{SO}_4$  and the solvent was removed under reduced pressure. The crude product was purified by column chromatography over silica gel, using gradient elution of 0-30% of ethyl acetate in hexane ( $v v^{-1}$ ) and 0-10% of methanol in ethyl acetate ( $v v^{-1}$ ).

#### 1-(2-(4-Phenyl-1*H*-1,2,3-triazol-1-yl)ethyl)piperidin-4-one (**4a**)

White solid, 61% yield, m.p. 113.9-115.4 °C;  $^1\text{H}$  NMR (400 MHz,  $\text{CDCl}_3$ )  $\delta$  7.92 (s, 1H), 7.86-7.84 (m, 2H), 7.46-7.42 (m, 2H), 7.37-7.28 (m, 1H), 4.59 (t,  $J$  6.0, 2H), 3.06 (t,  $J$  6.0, 2H), 2.87 (t,  $J$  6.0, 2H), 2.47 (t,  $J$  6.0, 2H);  $^{13}\text{C}$  NMR (100 MHz,  $\text{CDCl}_3$ )  $\delta$  207.8, 130.7, 129.0 (2C), 128.3, 125.8 (2C), 120.2, 56.6, 53.2 (2C), 48.3, 41.1 (2C); HRMS (ESI)  $m/z$ , calcd. for  $\text{C}_{15}\text{H}_{18}\text{N}_4\text{O}$  [ $\text{M} + \text{H}$ ] $^+$ : 271.15142, found: 271.15534.

#### *tert*-Butyl ((1-(2-(4-oxopiperidin-1-yl)ethyl)-1*H*-1,2,3-triazol-4-yl)methyl)carbamate (**4b**)

Yellow solid, 54% yield, m.p. 122.6-124.7 °C;  $^1\text{H}$  NMR (400 MHz,  $\text{CDCl}_3$ )  $\delta$  7.7 (s, 1H), 4.5 (t,  $J$  6.0, 2H), 4.4 (d,  $J$  6.0, 2H), 3.0 (t,  $J$  6.0, 2H), 2.8 (t,  $J$  6.0, 2H), 2.4 (t,  $J$  6.0, 2H), 1.4 (s, 9H);  $^{13}\text{C}$  NMR (100 MHz,  $\text{CDCl}_3$ )  $\delta$  208.0, 155.9, 145.5, 122.6, 79.7, 56.4, 53.0 (2C), 48.2, 41.0 (2C), 36.1, 28.4 (3C); HRMS (ESI)  $m/z$ , calcd. for  $\text{C}_{15}\text{H}_{25}\text{N}_4\text{O}_3$  [ $\text{M} + \text{H}$ ] $^+$ : 324.20302, found: 324.20252.

#### 1-(2-(4-((Naphthalen-1-yloxy)methyl)-1*H*-1,2,3-triazol-1-yl)ethyl)piperidin-4-one (**4c**)

Yellow oil, 57% yield;  $^1\text{H}$  NMR (400 MHz,  $\text{CDCl}_3$ )  $\delta$  7.70-7.64 (m, 4H), 7.38-7.44 (m, 1H), 7.28-7.25 (m, 1H), 7.19-7.18 (m, 1H), 7.12-7.09 (m, 1H), 5.28 (s, 2H), 4.47-4.44 (t, 2H), 2.93-2.90 (t, 2H), 2.72-2.69 (t, 4H), 2.30-2.27 (t, 4H);  $^{13}\text{C}$  NMR (100 MHz,  $\text{CDCl}_3$ )  $\delta$  207.3, 156.0, 144.2, 134.4, 129.6, 129.2, 127.7, 126.8, 126.6, 124.0, 123.4, 118.8, 107.3, 62.0 (2C), 56.3, 53.0 (2C), 48.1, 40.7; HRMS (ESI)  $m/z$ , calcd. for  $\text{C}_{20}\text{H}_{22}\text{N}_4\text{O}_2$  [ $\text{M} + \text{H}$ ] $^+$ : 351.17763, found: 351.19060.

#### 1-(2-(4-((3-Methoxyphenoxy)methyl)-1*H*-1,2,3-triazol-1-yl)ethyl)piperidin-4-one (**4d**)

Colorless oil, 76% yield;  $^1\text{H}$  NMR (400 MHz,  $\text{CDCl}_3$ )  $\delta$  7.70 (s, 1H), 7.20-7.10 (m, 1H), 6.60-6.50 (m, 3H), 5.20 (s, 2H), 4.50 (t,  $J$  6.0, 2H), 3.75 (s, 3H), 2.90 (t,  $J$  6.0, 2H), 2.80 (t,  $J$  6.0, 2H), 2.40 (t,  $J$  6.0, 2H);  $^{13}\text{C}$  NMR (100 MHz,  $\text{CDCl}_3$ )  $\delta$  208.0, 160.9, 159.4, 144.2, 130.0, 107.0, 106.8, 101.5, 62.1, 56.4 (2C), 55.4, 53.0, 48.3 (2C), 41.0; HRMS (ESI)  $m/z$ , calcd. for  $\text{C}_{17}\text{H}_{22}\text{N}_4\text{O}_3$  [ $\text{M} + \text{H}$ ] $^+$ : 331.17255, found: 331.18510.

#### 1-(2-(4-(3-Hydroxypropyl)-1*H*-1,2,3-triazol-1-yl)ethyl)piperidin-4-one (**4e**)

Colorless oil, 40% yield;  $^1\text{H}$  NMR (400 MHz,  $\text{CDCl}_3$ )  $\delta$  7.48 (s, 1H), 3.70 (t,  $J$  6.0, 2H), 4.48 (t,  $J$  6.0, 2H), 3.70 (t,  $J$  6.0, 2H), 3.00 (t,  $J$  6.0, 2H), 2.84-2.80 (m, 4H), 1.94 (q,  $J$  6.0, 2H);  $^{13}\text{C}$  NMR (100 MHz,  $\text{CDCl}_3$ )  $\delta$  208.3, 147.6, 121.6, 61.6, 56.5 (2C), 53.1, 48.2 (2C), 41.1, 32.1, 22.1; HRMS (ESI)  $m/z$ , calcd. for  $\text{C}_{12}\text{H}_{20}\text{N}_4\text{O}_3$  [ $\text{M} + \text{H}$ ] $^+$ : 253.16198, found: 253.16624.

#### General procedures for the synthesis of amines **5a-5e**

Aniline (1.0 equiv.) was taken up in  $\text{CH}_2\text{Cl}_2$  (5 mL) in a round-bottom flask equipped with a stir bar. The solution was treated dropwise with acetic acid (1.0 equiv.) To the mixture, a solution of the corresponding amine (**4a-4e**) (1.0 equiv.) in  $\text{CH}_2\text{Cl}_2$  (60 mL) was added, followed by the slow addition of sodium triacetoxyborohydride

(1.5 equiv.) in small portions. The reaction mixture was stirred under reflux for 20 h. After this time, the mixture was cooled to room temperature and extracted with saturated  $\text{NaHCO}_3$  (10 mL) and  $\text{CH}_2\text{Cl}_2$  (3  $\times$  10 mL). The organic layers were combined, dried with  $\text{Na}_2\text{SO}_4$  and the solvent was removed under reduced pressure. The solid mixture was purified by column chromatography using gradient elution of 70-90% of ethyl acetate in hexane ( $v v^{-1}$ ) and 0-10% of methanol in ethyl acetate ( $v v^{-1}$ ) to give compounds **5a-5e**.

*N*-Phenyl-1-(2-(4-phenyl-1*H*-1,2,3-triazol-1-yl)ethyl)piperidin-4-amine (**5a**)

Yellow solid, 54% yield, m.p. 119.2-121.5 °C;  $^1\text{H}$  NMR (400 MHz,  $\text{CDCl}_3$ )  $\delta$  7.91 (s, 1H), 7.85-7.83 (m, 2H), 7.45-7.41 (m, 2H), 7.37-7.29 (m, 1H), 7.18-7.14 (m, 2H), 6.73-6.65 (m, 1H), 6.60-6.58 (m, 2H), 4.51 (t,  $J$  6.0, 2H), 3.35-3.30 (septet, 1H), 2.89-2.87 (m, 2H), 2.32-2.29 (m, 1H), 2.09-2.06 (m, 1H), 1.51-1.42 (m, 1H);  $^{13}\text{C}$  NMR (100 MHz,  $\text{CDCl}_3$ )  $\delta$  147.8, 147.1, 130.9, 129.5 (2C), 129.0 (2C), 128.2, 125.8 (2C), 120.3, 117.5, 113.4 (2C), 57.7, 52.6, 49.8, 48.2, 32.7; HRMS (ESI)  $m/z$ , calcd. for  $\text{C}_{21}\text{H}_{25}\text{N}_5$  [ $\text{M} + \text{H}$ ] $^+$ : 348.21435, found: 348.21936.

*tert*-Butyl ((1-(2-(4-(phenylamino)piperidin-1-yl)ethyl)-1*H*-1,2,3-triazol-4-yl)methyl)carbamate (**5b**)

Yellow solid, 76% yield, m.p. 122.6-124.7 °C;  $^1\text{H}$  NMR (400 MHz,  $\text{CDCl}_3$ )  $\delta$  7.71 (s, 1H), 7.20-7.12 (m, 2H), 6.74-6.67 (m, 1H), 6.63-6.56 (m, 2H), 4.64-4.61 (m, 2H), 4.41-4.38 (m, 2H), 3.44-3.33 (septet, 1H), 3.15-2.91 (m, 3H), 2.51-2.46 (m, 1H), 2.15-2.12 (m, 1H), 1.68-1.60 (m, 1H), 1.44 (s, 9H);  $^{13}\text{C}$  NMR (100 MHz,  $\text{CDCl}_3$ )  $\delta$  155.7, 146.7, 129.5 (2C), 122.9, 117.9, 113.6 (2C), 79.9, 56.9, 52.3, 47.1, 36.3, 31.4, 28.5; HRMS (ESI)  $m/z$ , calcd. for  $\text{C}_{21}\text{H}_{32}\text{N}_6\text{O}_2$  [ $\text{M} + \text{H}$ ] $^+$ : 401.26203, found: 401.26595.

1-(2-(4-((Naphthalen-1-yloxy)methyl)-1*H*-1,2,3-triazol-1-yl)ethyl)-*N*-phenylpiperidin-4-amine (**5c**)

Yellow oil, 65% yield;  $^1\text{H}$  NMR (400 MHz,  $\text{CDCl}_3$ )  $\delta$  7.81-7.76 (m, 4H), 7.49-7.45 (m, 1H), 7.39-7.36 (m, 1H), 7.30-7.28 (m, 1H), 7.23-7.17 (m, 3H), 6.74-6.70 (m, 1H), 6.60-6.58 (m, 2H), 5.38 (s, 2H), 4.53-4.50 (t, 2H), 3.31-3.24 (septet, 1H), 2.90-2.83 (m, 4H), 2.29-2.24 (m, 2H), 2.00-1.97 (m, 2H), 1.39-1.32 (m, 2H);  $^{13}\text{C}$  NMR (100 MHz,  $\text{CDCl}_3$ )  $\delta$  156.1, 146.9, 144.0, 134.4, 129.6, 129.4 (2C), 129.2, 127.7, 127.0, 126.5, 124.0, 123.6, 118.9, 117.4, 113.3, 107.3, 62.1 (2C), 57.3, 52.4 (2C), 47.8, 32.1; HRMS (ESI)  $m/z$ , calcd. for  $\text{C}_{26}\text{H}_{29}\text{N}_5\text{O}$  [ $\text{M} + \text{H}$ ] $^+$ : 428.24057, found: 428.24449.

1-(2-(4-((3-Methoxyphenoxy)methyl)-1*H*-1,2,3-triazol-1-yl)ethyl)-*N*-phenylpiperidin-4-amine (**5d**)

Colorless oil, 45% yield;  $^1\text{H}$  NMR (400 MHz,  $\text{CDCl}_3$ )  $\delta$  7.76 (s, 1H), 7.21-7.15 (m, 3H), 6.72-6.70 (m, 1H), 6.68-6.53 (m, 5H), 5.23 (s, 2H), 4.49 (t,  $J$  6.0, 2H), 3.78 (s, 3H), 3.35-3.23 (m, 1H), 2.27-2.24 (m, 2H), 2.87-2.83 (m, 3H), 2.05-2.02 (m, 1H), 1.42-1.39 (m, 1H);  $^{13}\text{C}$  NMR (100 MHz,  $\text{CDCl}_3$ )  $\delta$  161.0, 159.6, 147.1, 144.1, 130.1, 129.5, 123.5, 177.5, 113.4, 107.1, 107.0, 101.5, 62.20, 55.4, 57.5, 52.5, 49.7, 48.0, 32.5; HRMS (ESI)  $m/z$ , calcd. for  $\text{C}_{23}\text{H}_{29}\text{N}_5\text{O}_2$  [ $\text{M} + \text{H}$ ] $^+$ : 408.23940; found: 408.23940.

3-(1-(2-(4-(Phenylamino)piperidin-1-yl)ethyl)-1*H*-1,2,3-triazol-4-yl)propan-1-ol (**5e**)

Colorless oil, 47% yield;  $^1\text{H}$  NMR (400 MHz,  $\text{CDCl}_3$ )  $\delta$  7.47 (s, 1H), 7.25-7.04 (m, 2H), 6.79-6.63 (m, 1H), 6.63-6.50 (m, 2H), 4.48 (t,  $J$  6.0, 2H), 3.71 (t,  $J$  6.0, 2H), 3.31-3.33 (m, 1H), 2.90-2.82 (m, 7H), 2.33-2.28 (m, 2H), 2.09-2.06 (m, 2H), 1.97-1.94 (m, 2H), 1.53-1.51 (m, 2H);  $^{13}\text{C}$  NMR (100 MHz,  $\text{CDCl}_3$ )  $\delta$  147.5, 147.0, 129.5 (2C), 121.8, 117.6, 113.5 (2C), 62.0, 57.6, 52.6, 49.6, 47.8, 32.4, 32.1, 22.3; HRMS (ESI)  $m/z$ , calcd. for  $\text{C}_{18}\text{H}_{27}\text{N}_3\text{O}$  [ $\text{M} + \text{H}$ ] $^+$ : 330.22156, found: 330.22256.

General procedures for the synthesis of amides **6a-6e**

The corresponding synthesized amine (**5a-5e**) was dissolved in  $\text{CH}_2\text{Cl}_2$  (4 mL) in a round bottom flask equipped with a small stir bar and was reacted with diisopropylethylamine (2.0 equiv.). The solution was cooled with an ice bath and treated dropwise with propionyl chloride (2.0 equiv.). The resulting mixture was stirred for 7 h at room temperature. The mixture was transferred to a separatory funnel and partitioned ( $\text{CH}_2\text{Cl}_2/\text{H}_2\text{O}$ ). The organic phase was washed with brine (15 mL), saturated  $\text{NaHCO}_3$  (15 mL), dried over  $\text{Na}_2\text{SO}_4$  and concentrated under reduced pressure to give the crude products that were purified by column chromatography using gradient elution of 30-70% of ethyl acetate in hexane ( $v v^{-1}$ ) to furnish the novel triazoles (**6a-6e**).

*N*-Phenyl-*N*-(1-(2-(4-phenyl-1*H*-1,2,3-triazol-1-yl)ethyl)piperidin-4-yl)propionamide (**6a**)

White solid, 52% yield, m.p. 120.5-122.4 °C;  $^1\text{H}$  NMR (400 MHz,  $\text{CDCl}_3$ )  $\delta$  7.80 (s, 1H), 7.74-7.72 (m, 2H), 7.44-7.74 (m, 2H), 7.44-7.34 (m, 2H), 7.34-7.27 (m, 1H), 7.07-7.04 (m, 2H), 4.48 (t,  $J$  6.0, 2H), 2.94-2.87 (m, 3H), 2.36-2.30 (m, 1H), 1.91 (t,  $J$  8.0, 3H) 1.81-1.78 (m, 1H), 1.47-1.41 (m, 1H), 0.99 (q,  $J$  8.0, 2H);  $^{13}\text{C}$  NMR (100 MHz,  $\text{CDCl}_3$ )  $\delta$  173.7, 147.6, 138.8, 130.7, 130.3, 128.9 (2C), 128.6 (2C), 128.2 (2C), 125.7 (2C), 120.4, 57.2, 53.2 (2C),

51.2, 47.2, 30.3 (2C), 28.6, 9.7; HRMS (ESI)  $m/z$ , calcd. for  $C_{24}H_{29}N_5O$  [M + H]<sup>+</sup>, 404.24057; found 404.24449.

*tert*-Butyl ((1-(2-(4-(*N*-phenylpropionamido)piperidin-1-yl)ethyl)-1*H*-1,2,3-triazol-4-yl)methyl)carbamate (**6b**)

White solid, 49% yield, m.p. 110.3-112.1 °C; <sup>1</sup>H NMR (400 MHz, CDCl<sub>3</sub>) δ 7.54 (s, 1H), 7.09-7.06 (m, 5H), 4.65 (tt, *J* 12.0, 4.0, 1H), 4.43 (t, *J* 6.0, 2H), 4.34 (s, 2H), 2.94-2.85 (m, 3H), 2.33-2.30 (m, 1H), 1.91 (q, *J* 8.0, 2H), 1.84-1.73 (m, 1H), 1.50-1.35 (m, 10H), 1.01 (t, *J* 8.0, 3H); <sup>13</sup>C NMR (100 MHz, CDCl<sub>3</sub>) δ 173.7, 155.9, 145.4, 138.8, 130.3 (2C), 129.6 (2C), 128.6, 122.4, 79.7, 57.3, 53.3 (2C), 51.9, 47.6, 36.2, 30.2 (2C), 28.6, 28.5 (3C), 9.7; HRMS (ESI)  $m/z$ , calcd. for  $C_{24}H_{36}N_6O_3$  [M + H]<sup>+</sup>: 457.29217, found: 457.29132.

*N*-(1-(2-(4-((3-Methoxyphenoxy)methyl)-1*H*-1,2,3-triazol-1-yl)ethyl)piperidin-4-yl)-*N*-phenylpropionamide (**6c**)

Colorless oil, 48% yield; <sup>1</sup>H NMR (400 MHz, CDCl<sub>3</sub>) δ 7.76 (s, 1H), 7.21-7.15 (m, 3H), 6.72-6.70 (m, 1H), 6.68-6.53 (m, 5H), 2.23 (s, 3H), 4.49 (t, *J* 6.0, 2H), 3.35-3.23 (m, 1H), 2.87-2.83 (m, 3H), 2.27-2.24 (m, 1H), 2.05-2.02 (m, 1H), 1.42-1.39 (m, 1H); <sup>13</sup>C NMR (100 MHz, CDCl<sub>3</sub>) δ 173.7, 161.0, 159.6, 144.1, 139, 130.4 (2C), 130.0, 129.5 (2C), 128.5, 123.2, 106.9, 101.5, 62.2, 57.5, 55.4, 53.3 (2C), 52.2, 48.1, 30.6 (2C), 28.6, 9.7; HRMS (ESI)  $m/z$ , calcd. for  $C_{29}H_{33}N_5O_2$  [M + H]<sup>+</sup>: 464.26560, found: 464.27460.

*N*-(1-(2-(4-((Naphthalen-1-yloxy)methyl)-1*H*-1,2,3-triazol-1-yl)ethyl)piperidin-4-yl)-*N*-phenylpropionamide (**6d**)

Yellow oil, 65% yield; <sup>1</sup>H NMR (400 MHz, CDCl<sub>3</sub>) δ 7.77-7.72 (m, 4 H), 7.45-7.32 (m, 5H), 7.24-7.23 (m, 1H), 7.15-7.12 (m, 1H), 7.05-7.03 (m, 1H), 5.35 (s, 2H), 4.66-4.60 (m, 1H), 4.51-4.48 (m, 2H), 2.92-2.91 (m, 2H), 2.36-2.24 (m, 2H), 1.91 (q, *J* 6.0, 2H), 1.78-1.74 (m, 2H), 1.48-1.39 (m, 2H), 1.00 (t, *J* 6.0, 3H); <sup>13</sup>C NMR (100 MHz, CDCl<sub>3</sub>) δ 173.7, 156.1, 134.4, 130.2 (2C), 129.5, 129.4, 127.6, 126.9, 123.9, 116.8, 107.3, 62.0 (2C), 56.9, 53.1 (2C), 47.3, 29.8, 28.5, 9.6; HRMS (ESI)  $m/z$ , calcd. for  $C_{29}H_{33}N_5O_3$  [M + H]<sup>+</sup>: 484.27830, found: 464.27460.

3-(1-(2-(4-(*N*-Phenylpropionamido)piperidin-1-yl)ethyl)-1*H*-1,2,3-triazol-4-yl)propyl propionate (**6e**)

Colorless oil, 50% yield; <sup>1</sup>H NMR (400 MHz, CDCl<sub>3</sub>) δ 7.48 (s, 1H), 7.48-7.32 (m, 3H), 7.14-6.99 (m 2H), 4.62 (tt, *J* 12.0, 4.0), 4.49-4.36 (m, 2H), 4.09 (t, *J* 6.0, 2H), 3.00-2.81 (m, 3H), 2.20-2.81 (m, 3H), 2.75 (t, *J* 6.0, 3H), 2.01-1.85 (m, 4H), 1.85-1.72 (m, 1H), 1.58-1.35 (m, 1H), 1.16 (t, *J* 6.0, 3H), 1.0 (t, *J* 6.0, 3H); <sup>13</sup>C NMR (100 MHz, CDCl<sub>3</sub>) δ 174.6, 173.8, 157.4, 147.1, 138.8, 130.3 (2C), 129.6 (2C), 128.6, 128.5, 121.7, 63.46, 57.2, 53.3 (2C),

51.7, 47.3, 30.0 (2C), 28.6, 28.5, 27.7, 22.2, 9.7, 9.3; HRMS (ESI)  $m/z$ , calcd. for  $C_{24}H_{35}N_5O_3$  [M + H]<sup>+</sup>: 442.28127, found: 442.28066.

## Biological evaluations

### Cell culture

Human lung cell line A549 was purchased from the American Type Culture Collection (Manassas, Virginia, United States). The lung cell line was cultured in F12K medium (Corning, New York, United States) supplemented with 10% fetal bovine serum from CytoGen (Princeton, New Jersey, United States) and 1% penicillin-streptomycin (Corning, New York, United States). The hMOR-CHO cells overexpressing the human MOR receptor was a generous gift from Prof Anna Janecka (Department of Medicinal Chemistry, Medical University of Lodz, Lodz, Poland) were cultured in Ham's F12 medium (Corning, New York, United States) supplemented with 10% fetal bovine serum from CytoGen (Princeton, New Jersey, United States) and 400 µg mL<sup>-1</sup> G418 (Corning, New York, United States). All cell lines were kept at 37 °C under a humidified atmosphere with 5% CO<sub>2</sub>.

### hMOR-CHO membrane preparation

The hMOR-CHO cells were harvested with 0.05% trypsin/EDTA (Corning, New York, United States) and centrifuged at 1500 rpm for 5 min. The pellets were homogenized by using a glass tissue homogenizer in an ice-cold 50 mM Tris HCl (pH 7.4) buffer. The preparation was centrifuged at 13,000 rpm for 25 min at 4 °C and the pellets containing the membrane fractions were collected, pulled together and suspended in the buffer. 500 µL aliquots of the homogenates were stored at -80 °C for later use. The amount of protein in the homogenates was determined by the bicinchonic acid (BCA) method of Thermo Scientific (Waltham, Massachusetts, United States). On the day of the experiment, the homogenate portions were thawed and suspended in 50 mM Tris-HCl (pH 7.4).

### A549 membrane preparation

The A549 cells were harvested with 0.25% trypsin/EDTA (Corning, New York, USA) and centrifuged at 1500 rpm for 5 min. The pellets were homogenized by using a glass tissue homogenizer in an ice-cold 50 mM Tris HCl (pH 8.0) buffer. The preparation was centrifuged at 13,000 rpm for 25 min at 4 °C and the pellets containing the membrane fractions were collected, pulled together and suspended in the buffer. 500 µL aliquots of the homogenates were stored at -80 °C for later use. The amount of protein in the homogenates was determined by the BCA method of Thermo Scientific

(Waltham, Massachusetts, United States). On the day of the experiment, the homogenate portions were thawed and suspended in 50 mM Tris-HCl (pH 8.0).

#### Receptor binding affinity assay

The binding affinity of the tested compounds for human MOR was determined in competitive radioligand binding assays. Homogenates made from CHO-MOR cells were used. The membrane preparations were incubated at 25 °C for 60 min in the presence of 1 nM [tyrosyl-3,5-3H(*N*)]-DAMGO from PerkinElmer (Boston, Massachusetts, United States) and appropriate concentrations of the assayed compound. Non-specific binding was measured in the presence of 10 µM naltrexone from Sigma-Aldrich (St. Louis, Missouri, United States). The assays were conducted with the assay buffer made of 50 mM Tris-HCl (pH 7.4). The total reaction volumes were 250 µL. For the assays with σ1R, homogenates made from A549 lung cells were used. The membrane preparations were incubated at 37 °C for 90 min in the presence of 1 nM [RING-1,33H]-Pentazocine from PerkinElmer, (Boston, Massachusetts, United States) and appropriate concentrations of the assayed compound. Non-specific binding was measured in the presence of 10 µM SK&F10047 from Tocris (Abingdom, United Kingdom). The assays were conducted with the assay buffer made of 50 mM Tris-HCl (pH 8.0). The total reaction volumes were 250 µL. In order to terminate the binding reaction, a rapid filtration with a M-24 Cell Harvester from Brandel (Gaithersburg, Maryland, United States) through GF/B Whatman filter was performed. The filters were pre-soaked with 0.5% polyethylenimine (PEI) for minimizing the extent of non-specific binding. Filter discs were placed in 24-well plates and a Betaplate Scint scintillation solution from PerkinElmer (Boston, Massachusetts, United States) was added to each well. Radioactivity was measured in a scintillation counter MicroBeta LS, Trilux from PerkinElmer (Boston, Massachusetts, United States). The displacement curves were drawn and the mean half-maximal inhibitory concentrations (IC<sub>50</sub>) values were determined with standard deviations by GraphPad Prism (GraphPad Software Inc.).<sup>26</sup>

#### ADMET prediction

Prediction of absorption, distribution, metabolism, and excretion toxicity (ADMET) parameters for compounds **6a-6e** was carried out using the SwissADME tool.<sup>27</sup> The service provides a set of fast and robust models for physicochemical properties, pharmacokinetic behavior,

druglikeness and leadlikeness based on validated and commonly accepted algorithms.

#### Molecular modelling

Molecular docking was performed in AutoDock 4.2.6. using the Lamarckian Genetic algorithm as a search method.<sup>28</sup> The structures of **6a-6e** were optimized at the B3LYP/6-31G(d,p) level in Gaussian09.<sup>29</sup> 5HK2 structure was used for docking to σ1R. In docking simulations, Asp126 of σ1R was kept protonated and H-bonded to Glu172. In the case of MOR, the receptor structure was a snapshot from the molecular dynamics simulations of 5C1M MOR structure bound to fentanyl.<sup>30</sup> We used this structure as we feel it suitable for modelling fentanyl analogues with MOR. The docking boxes were set to encompass the binding sites of MOR and σ1R but significantly extended (box sizes: MOR 34 Å × 34 Å × 34 Å, σ1R 25 Å × 34 Å × 31 Å). The grids were calculated with AutoGrid 4.<sup>28</sup> Full ligand flexibility (except for amide bonds) was allowed. The receptor structures were treated as rigid. The docking parameters were population size 150, maximum number of energy evaluations 50000, maximum number of generations 3700, mutation rate 0.02, crossover rate 0.8, iterations of Solis & Wets local search 500, sw\_rho 5.0, number of hybrid genetic algorithm/local-search runs 300. The docking results were clustered, and structures from the best scored cluster were taken for further analyses. Molecular graphics was prepared in Biovia Discovery Studio Visualizer and in open-source PyMol.<sup>31,32</sup>

## Results and Discussion

### Chemistry

The novel fentanyl triazole analogues (**6a-6e**) were designed with the purpose to elucidate the effect of aromatic ring replacement in the phenylethyl group for another aromatic heterocycle ring. This strategy was used to provide analogues such as alfentanil (containing a tetrazole ring) and sulfentanil (a thiophene derivative). Once shortening the *N*-phenethyl chain results in a decrease of affinity, we chose to maintain the ethyl bridge between the triazole and the piperidine ring.<sup>9</sup> Thus, the synthesis of azide **2** was the key step to obtain the novel compounds (Scheme 1). This synthesis was made using a one pot methodology, with the addition of the 1-azido-2-bromoethane (obtained after 24 h stirring an excess of sodium azide salt with 1,2-dibromoethane) to the solution of 4-*N*-piperidone, in the presence of a mild base. The second step was to prepare 1,4-dissubstituted-

1,2,3-triazole analogues **3a-3e**. Different commercial alkynes were selected containing aromatic rings, aliphatic chain, ether and carbamate groups to accomplish the click reaction with azide **2**. The alkynes **3b**,<sup>33</sup> **3c**<sup>34</sup> and **3d**<sup>34</sup> were prepared according with methodologies already described in literature. The click reaction catalyst ( $\text{Cu}^+$ ) was obtained from the reduction of  $\text{Cu}^{2+}$ , from copper sulfate ( $\text{CuSO}_4$ ), by sodium ascorbate salt ( $\text{NaAsc}$ ) and furnished ketones **3a-3e**. The next steps to obtain the novel triazole analogues were the reductive amination of the carbonyl group to provide amines **4a-4e**, followed by acylation of the resulted secondary amines with propionyl chloride, yielding the novel analogues **5a-5e**, employing a methodology optimized by Valdez *et al.*<sup>35</sup> Compound **6e** was obtained by double acylation of compound **5e**.

### Receptor affinity

The target compounds were tested as to their MOR and  $\sigma$ 1R affinity. The binding data are given in Table 1. The novel triazoles exhibit moderate or very low affinity (in the micromolar range) for both receptors. The most active analogue is **6d** which binds to MOR with  $\text{IC}_{50} = 1.9 \mu\text{M}$  and to  $\sigma$ 1R with  $\text{IC}_{50} = 6.9 \mu\text{M}$ . Still, **6d** is weaker MOR binder than the parent fentanyl (by more than 1000-times) and then alfentanil (by about 50-times). In the case of  $\sigma$ 1R, **6d** binds slightly worse than the parent fentanyl and

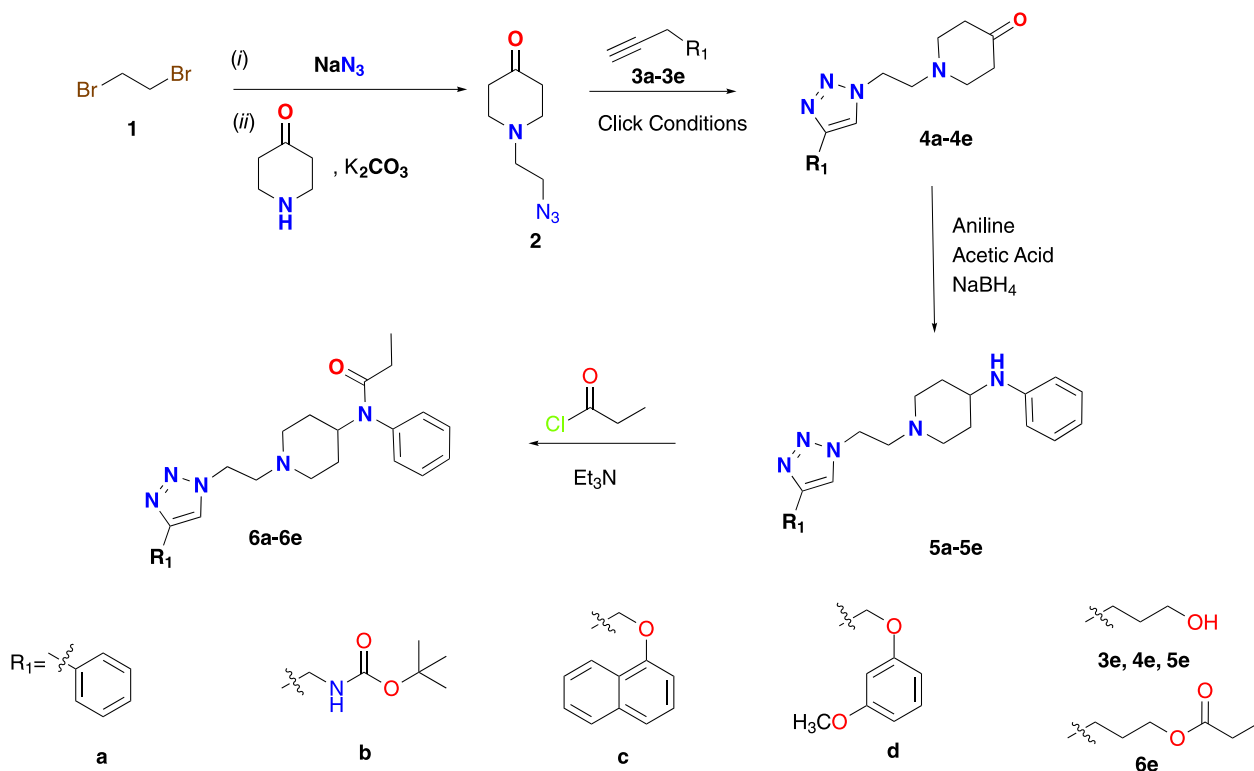
better than alfentanil, but significantly worse than reference SKF10047 or *N*-benzylfentanyl.

The values are mean half-maximal inhibitory concentrations ( $\text{IC}_{50}$ )  $\pm$  standard deviation, obtained from three independent experiments done in duplicate.

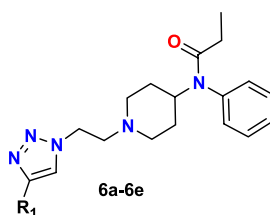
### Prediction of ADMET properties

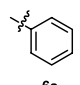
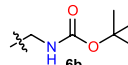
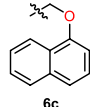
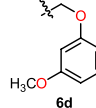
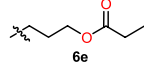
The ADMET properties of compounds **6a-6e** were predicted *in silico* using the SwissADME tool.<sup>27</sup> ADMET stands for absorption, distribution, metabolism, excretion, and toxicity. It is important to evaluate ADMET properties for new bioactive compounds since it helps to determine potential for their development as medicinal substances and to guide any further structural optimization. The results of the SwissADME predictions are given in detail in Supplementary Information (SI) section (Tables S1-S5). Their summary is presented in Figure 2 (bioavailability radar plot), Figure 3 (absorption prediction) and Table 2.

SwissADME evaluation points to rather good drug-like properties of our new triazoles, as most drug-likeness criteria are satisfied for all compounds. Worth noting is the good bioavailability score with the value of 0.55 (probability that the compound would have at least 10% oral bioavailability in rat or measurable Caco-2 permeability).<sup>37</sup> The compounds exhibit reasonable lipophilicity (consensus  $\text{LogP}_{\text{ow}}$ ) in the range of 1.81 (**6b**)-3.28 (**6c**).



**Scheme 1.** Synthesis route of novel triazole analogues of fentanyl **6a-6e**.

**Table 1.** Binding affinity for MOR and  $\sigma$ 1R


Compound	MOR IC <sub>50</sub> / $\mu$ M	$\sigma$ 1R IC <sub>50</sub> / $\mu$ M
Fentanyl	0.001 <sup>8</sup>	5.0 <sup>36</sup>
<i>N</i> -Benzyl fentanyl	0.489 <sup>8</sup>	0.322 <sup>36</sup>
Alfentanil	0.039 <sup>8</sup>	> 10 <sup>36</sup>
SKF10047	–	0.069
 <b>6a</b>	> 20	12.7 $\pm$ 6.8
 <b>6b</b>	4.5 $\pm$ 1.3	11.7 $\pm$ 4.4
 <b>6c</b>	> 20	11.2 $\pm$ 4.7
 <b>6d</b>	1.9 $\pm$ 0.4	6.9 $\pm$ 0.6
 <b>6e</b>	11.1 $\pm$ 6.5	25.0 $\pm$ 3.2

MOR: Mu-opioid receptor;  $\sigma$ 1R: sigma-1 receptor; IC<sub>50</sub>: half-maximal inhibitory concentrations.

All compounds are predicted to have high gastrointestinal absorption (Figure 3). Furthermore, **6a**, **6c** and **6d** are forecasted to passively permeate through the blood-brain barrier, which is favorable for compounds whose expected mechanism of action involves activity at the receptors distributed in the central nervous system. On the other hand, for the compound **6c** it is predicted that it might be a P-gp efflux substrate.

A potential toxic liability of the new compounds is their involvement as cytochrome P enzyme family inhibitors. SwissADME predicts that the new triazoles inhibit the CYP3A4 isoform. Additionally, CYP2C19 is predicted to be inhibited by **6a** and **6c**, while CYP2C9 to be inhibited by **6a**, **6c**, **6d**.

None of the compounds shows any problems according to Brenk<sup>38</sup> and PAINS<sup>39</sup> alert filter, meaning that they do not contain elements responsible for toxic, chemically reactive or metabolically unstable behavior.

Unfortunately, the new analogues do not fulfil lead-likeness criteria. It means that any further structural optimization should be restricted to molecular simplification and replacements while structural expansion should be avoided. In particular, as seen in Figure 2, molecular size (weight) and lipophilicity are near the high end of what is perceived as beneficial to good bioavailability. Moreover, molecular flexibility might be reduced to improve bioavailability.

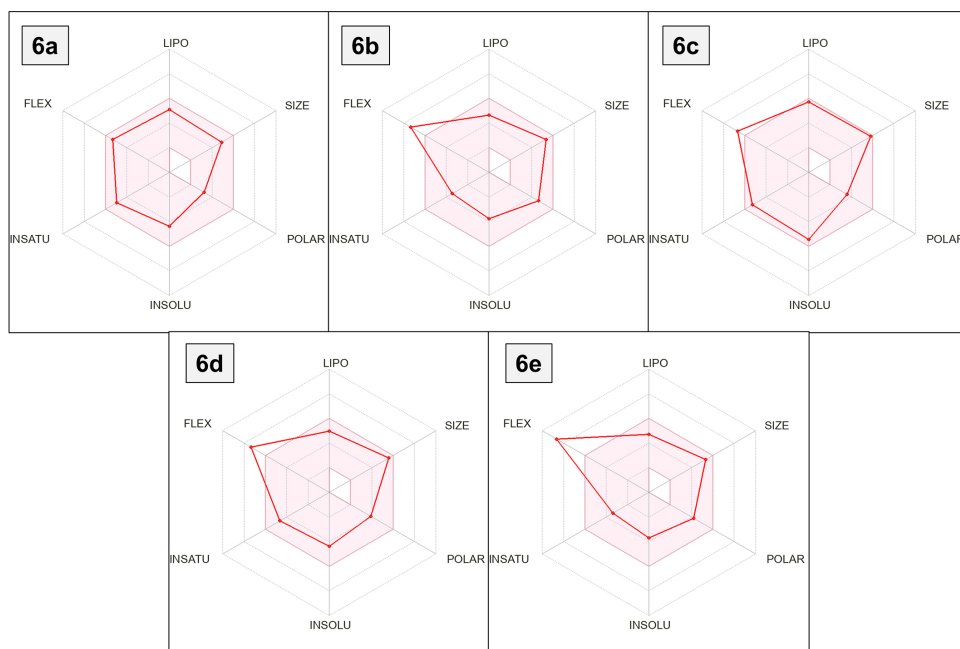


**Figure 2.** The bioavailability radar plots for compounds **6a-6e** predicted by the SwissADME tool. The prediction takes into account lipophilicity (LIPO), molecular size (SIZE), polarity (POLAR), solubility (INSOLU), flexibility (FLEX) and saturation (INSATU). The pink area represents the optimal range for each property.



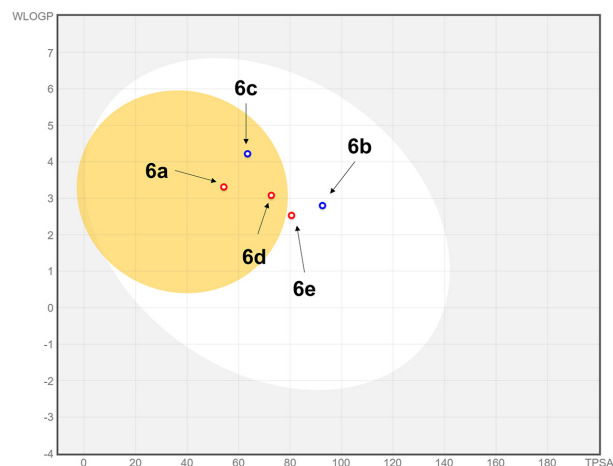


**Figure 3.** Absorption prediction for compounds **6a-6e** (according to the BOILED-Egg method). The points are colored according to the prediction whether the compound is (blue) or is not (red) a substrate for P-glycoprotein efflux. The points located in the yolk region are for the compounds predicted to passively permeate through the blood-brain barrier. The points located in the white region are the compounds predicted to be passively absorbed by the gastrointestinal tract. The yolk and white regions are not mutually exclusive. WLOGP: lipophilicity parameter, TPSA: topological polar surface area.

**Table 2.** Selected ADMET parameters for compounds **6a-6e** predicted *in silico* by SwissADME web-service

Test	<b>6a</b>	<b>6b</b>	<b>6c</b>	<b>6d</b>	<b>6e</b>
Consensus Log <sub>P<sub>o/w</sub></sub>	2.49	1.81	3.28	2.39	2.03
Water solubility	moderate to poor	moderate	moderate to poor	moderate to poor	moderate to poor
GI absorption	high	high	high	high	high
BBB permeation	yes	no	yes	yes	no
P-gp substrate	no	yes	yes	no	no
CYP inhibition	CYP2C19, CYP2C9, CYP3A4	CYP3A4	CYP2C19, CYP2C9, CYP3A4	CYP2C9, CYP3A4	CYP3A4
Bioavailability score	0.55	0.55	0.55	0.55	0.55
PAINS alert	no	no	no	no	no
Brenk alert	no	no	no	no	no

Log<sub>P<sub>o/w</sub></sub>: logarithm of partition coefficient between octanol and water; BBB: blood brain barrier; GI: gastrointestinal; P-gp: P-glycoprotein; CYP: cytochrome P; PAINS: Pan-assay interference compounds.

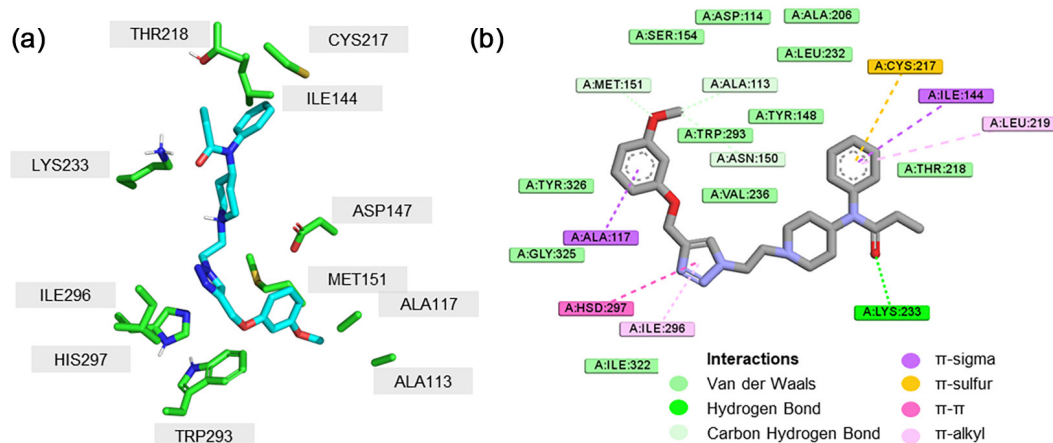


**Figure 4.** Interactions of compound **6d** with MOR binding site as found by docking. (a) View of **6d** in the binding site. (b) Scheme of interactions.

## Molecular modelling

In order to rationalize the observed affinities in terms of ligand-receptor interactions, the compounds **6a-6e** were modelled in the binding sites of receptors of interest. The docking poses at MOR binding site are shown in Figure 4 (compound **6d**) and Figures S48-S55 in SI section. The binding orientations of our triazoles are diversified (no common binding mode). The analogue **6d** is located with the triazole-bearing arm directed downwards to the bottom of the binding pocket. On the contrary, the analogues **6a**, **6b**, **6c** and **6e** have this element directed towards the extracellular outlet of the binding site.

The strongest MOR binder, compound **6d** exhibits a single H-bond between the propanilide carbonyl oxygen and Lys233 side chain. Other interactions stabilizing **6d** MOR complex include hydrophobic contacts of the anilide's phenyl ring with Ile144, Cys217 and Leu219 side-chains. The triazole ring is involved in stacking interaction with His297 and in other hydrophobic contacts to Ile296 side

chain. The 3-methoxyphenoxy-moiety is accommodated at the very bottom of the binding site, forming contacts among others Ala113, Ala117, Met151 and Trp293.

The other two MOR binders for which  $IC_{50}$ 's were determined (compounds **6b** and **6e**) do also exhibit a single H-bond to Lys233, while very poor binders **6a** and **6c** have no H-bond to MOR. The detailed schemes of their predicted interactions with MOR are shown in SI section (Figures S48-S55).

Overall, the results of docking are consistent with low or moderate MOR affinities of our triazoles. None of the compounds exhibits the canonical interaction between the protonated amine of the piperidine ring and the Asp147 side chain. This interaction is usually expected of high-affinity MOR ligands (as evidenced by mutagenetic<sup>40</sup> and crystallography).<sup>30,41,42</sup> This contact was also found for fentanyl and its analogues in previous *in silico* works of ours<sup>8</sup> and of other workers.<sup>43</sup> The presence of a single H-bond is seemingly not sufficient to provide strong binding, but it is sufficient (together with extensive hydrophobic contacts) to give micromolar affinity.

The predicted  $\sigma$ 1R binding modes of our triazoles are shown in Figure 5 (compound **6d**) and in Figures S56-S64 (SI section). All the compounds fit within the buried  $\beta$ -barell binding site filling it almost entirely (Figure S9). Strikingly, none of the compounds exhibit any H-bond to the binding site residues, and the complexes are stabilized exclusively with hydrophobic contacts.

Regarding the complex of the strongest  $\sigma$ 1R binder (compound **6d**), the anilide aromatic ring is inserted between the side chains of Leu95, Ala98, Tyr103, Leu105, Ile178 and Tyr206. The piperidine ring is wedged between Val84, Tyr103, Ala185. The protonated nitrogen is turned “downwards” away from Glu172 and does not form an interaction with this side chain. The triazole ring is predicted to  $\pi$ -stack with Trp89. The 3-methoxyphenoxy-

arm bends upwards to fill a subpocket delineated by Ile124, Asp126, Phe133, Val152, Val153 and His154. The interactions of the remaining analogues are shown in SI section (Figures S56-S64).

The docking results are consistent with low but measurable  $\sigma$ 1R binding of our triazoles. On the one hand, the extensive hydrophobic contacts predicted for our triazoles provide stabilization to the complexes. On the other hand, lack of the interaction with Glu172 (or any other H-bond) does not allow for reaching nanomolar binding. An H-bond between the protonated nitrogen and Glu172 is a pharmacophoric interaction for strong  $\sigma$ 1R ligands and this interaction is present in crystallographic structures of the receptor.<sup>28,44</sup>

In outlook, in the reported research we wanted to see if it is possible to merge triazole moiety into the structure of fentanyl. The current work was focused on installing this heterocycle into the B-region of this structure (Figure 1). Experimental data on receptor affinity show that this attempt was moderately successful yielding compounds that exhibit binding to both MOR and  $\sigma$ 1R; however much lower than that found for reference ligands. This is in contrast to very potent fentanyl analogues, like sufentanil or alfentanil which also contain heterocycles in region B (Figure 1).<sup>8</sup> On the other hand, those compounds have also other substituents that provide anchoring points for ligand-receptor interactions. The modelling presented in this work for the triazole fentanyl analogues provides a rational way to modify the reported molecules to improve their affinities.

Furthermore, it might be desirable to install triazole fragment onto other parts of the fentanyl structure, e.g., region C and D. In a recent work by Levoine *et al.*,<sup>45</sup> *N*-benzyl-piperidines substituted in position 4 with 1,2,3-triazoles were shown to be potent dual dopamine D4/sigma  $\sigma$ 1 receptor ligands.<sup>45</sup> Another recent research relevant to our work is that by Díaz *et al.*<sup>46</sup> who found tricyclic triazoles as potent

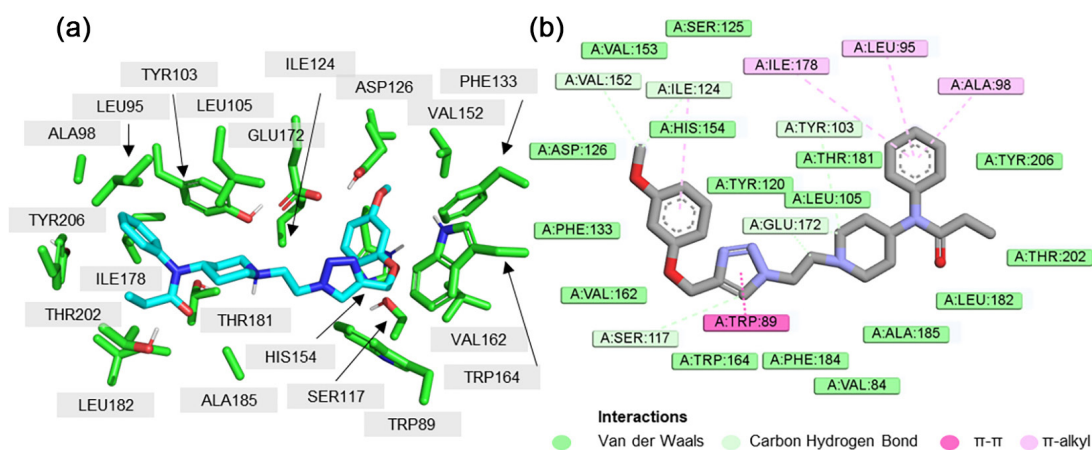


**Figure 5.** Interactions of compound **6d** with  $\sigma$ 1R binding site as found by docking. (a) View of **6d** in the binding site. (b) Scheme of interactions.

$\sigma$ 1 receptor antagonists with very good analgesic properties. Given high potential of the fentanyl structure as an interesting scaffold for developing multitarget analgesic compounds<sup>47</sup> and the recent interest in such compounds with  $\sigma$ 1 receptor component profile<sup>48-50</sup> further attempts to devise novel active fentanyl-related triazoles with are warranted.

## Conclusions

In summary, herein we reported the synthesis and binding assays of five new analogues of fentanyl containing a triazole ring. The compounds presented lower affinity to the MOR receptor when compared to fentanyl, but they showed a similar value of binding to the  $\sigma$ 1R. The compound **6d** was the most active analogue of the series (MOR IC<sub>50</sub> = 1.9  $\mu$ M and  $\sigma$ 1R IC<sub>50</sub> = 6.9  $\mu$ M) and the docking study showed that the observed result is related to the interaction between the single H-bond of propanilide carbonyl oxygen and Lys233 side chain. The results presented in this work are relevant since it is presented for the first-time binding assays of a triazole derivative of fentanyl towards the  $\sigma$ 1R. Therefore, further studies will be carried out to evaluate the structure activity of other triazole analogues of fentanyl in order to improve their affinity to the MOR and  $\sigma$ 1R receptors.

## Supplementary Information

Supplementary information is available free of charge at <http://jbcs.sbq.org.br> as PDF file.

## Acknowledgments

RPP, RBA and RPF acknowledge grants from the Conselho Nacional de Desenvolvimento Científico e Tecnológico (Brazil). The authors wish to thank FAPEMIG for financial support (APQ02389-17). Piotr F.J. Lipiński acknowledges the institutional grant at Mossakowski Medical Research Institute PAS (grant No. FBW-010). The molecular modelling was performed using the resources of the Świerk Computing Centre, National Centre for Nuclear Research, Świerk, Poland.

## References

1. Zhuang, T.; Xiong, J.; Hao, S.; Du, W.; Liu, Z.; Liu, B.; Zhang, G.; Chen, Y.; *Eur. J. Med. Chem.* **2021**, *223*, 113658. [Crossref]
2. Goldberg, D. S.; McGee, S. J.; *BMC Public Health* **2011**, *11*, 770. [Crossref]
3. Stein, C.; Küchler, S.; *Trends Pharmacol. Sci.* **2013**, *34*, 303. [Crossref]
4. Olkkola, K. T.; Kontinen, V. K.; Saari, T. I.; Kalso, E. A.; *Trends Pharmacol. Sci.* **2013**, *34*, 206. [Crossref]
5. The Lancet Public Health; *Lancet Public Health* **2022**, *7*, e195. [Crossref]
6. Stanley, T. H.; *J. Pain* **2014**, *15*, 1215. [Crossref]
7. Vardanyan, R. S.; Hrubby, V. J.; *Future Med. Chem.* **2014**, *6*, 385. [Crossref]
8. Lipiński, P. F. J.; Kosson, P.; Matalińska, J.; Roszkowski, P.; Czarnocki, Z.; Jarończyk, M.; Misicka, A.; Dobrowolski, J. C.; Sadlej, J.; *Molecules* **2019**, *24*, 740. [Crossref]
9. Dosen-Micovic, L.; Ivanovic, M.; Micovic, V.; *Bioorg. Med. Chem.* **2006**, *14*, 2887. [Crossref]
10. Gilbert, P. E.; Martin, W. R.; *J. Pharmacol. Exp. Ther.* **1976**, *198*, 66.
11. Su, T. P.; *J. Pharmacol. Exp. Ther.* **1982**, *223*, 284.
12. Nguyen, L.; Lucke-Wold, B. P.; Mookerjee, S. A.; Cavendish, J. Z.; Robson, M. J.; Scandinaro, A. L.; Matsumoto, R. R.; *J. Pharmacol. Sci.* **2015**, *127*, 17. [Crossref]
13. Su, T.-P.; Su, T.-C.; Nakamura, Y.; Tsai, S.-Y.; *Trends Pharmacol. Sci.* **2016**, *37*, 262. [Crossref]
14. Maurice, T.; Su, T.-P.; *Pharmacol. Ther.* **2009**, *124*, 195. [Crossref]
15. Cobos, E.; Entrena, J.; Nieto, F.; Cendan, C.; Del Pozo, E.; *Curr. Neuropharmacol.* **2009**, *6*, 344. [Crossref]
16. Narayanan, S.; Bhat, R.; Mesangeau, C.; Poupaert, J. H.; McCurdy, C. R.; *Future Med. Chem.* **2011**, *3*, 79. [Crossref]
17. Sambo, D. O.; Lebowitz, J. J.; Khoshbouei, H.; *Pharmacol. Ther.* **2018**, *186*, 152. [Crossref]
18. Fallica, A. N.; Pittalà, V.; Modica, M. N.; Salerno, L.; Romeo, G.; Marrazzo, A.; Helal, M. A.; Intagliata, S.; *J. Med. Chem.* **2021**, *64*, 7926. [Crossref]
19. Bruna, J.; Videla, S.; Argyriou, A. A.; Velasco, R.; Villoria, J.; Santos, C.; Nadal, C.; Cavaletti, G.; Alberti, P.; Briani, C.; Kalofonos, H. P.; Cortinovis, D.; Sust, M.; Vaqué, A.; Klein, T.; Plata-Salamán, C.; *Neurotherapeutics* **2018**, *15*, 178. [Crossref]
20. Villard, V.; Espallergues, J.; Keller, E.; Vamvakides, A.; Maurice, T.; *J. Psychopharmacol.* **2011**, *25*, 1101. [Crossref]
21. Prezzavento, O.; Arena, E.; Sánchez-Fernández, C.; Turnaturi, R.; Parenti, C.; Marrazzo, A.; Catalano, R.; Amata, E.; Pasquinucci, L.; Cobos, E. J.; *Eur. J. Med. Chem.* **2017**, *125*, 603. [Crossref]
22. García, M.; Virgili, M.; Alonso, M.; Alegret, C.; Farran, J.; Fernández, B.; Bordas, M.; Pascual, R.; Burgueño, J.; Vidal-Torres, A.; Fernández De Henestrosa, A. R.; Ayet, E.; Merlos, M.; Vela, J. M.; Plata-Salamán, C. R.; Almansa, C.; *J. Med. Chem.* **2020**, *63*, 15508. [Crossref]
23. García, M.; Virgili, M.; Alonso, M.; Alegret, C.; Fernández, B.; Port, A.; Pascual, R.; Monroy, X.; Vidal-Torres, A.; Serafini, M. T.; Vela, J. M.; Almansa, C.; *J. Med. Chem.* **2020**, *63*, 2434. [Crossref]
24. Nami, M.; Salehi, P.; Bararjanian, M.; Delshad, N. S.; Heidari,

- B.; Khoramjouy, M.; Shahhosseini, S.; Faizi, M.; *Med. Chem. Res.* **2022**, *31*, 886. [Crossref]
25. Reis, W. J.; Moreira, P. O. L.; Alves, R. B.; Oliveira, H. H. M.; Silva, L. M.; Varotti, F. P.; Freitas, R. P.; *Curr. Top. Med. Chem.* **2018**, *18*, 1475. [Crossref]
26. Motulsky, H.; *GraphPad Prism*, Inc., v. 5.0; Software Mackiey, San Diego, CA, USA, 2012.
27. SwissADME, <http://www.swissadme.ch/>, accessed in March 2023.
28. Morris, G. M.; Huey, R.; Lindstrom, W.; Sanner, M. F.; Belew, R. K.; Goodsell, D. S.; Olson, A. J.; *Autodock* version 4.2; University of California, San Diego, CA, USA, 2009.
29. Frisch, M. J.; Trucks, G. W.; Schlegel, H. B.; Scuseria, G. E.; Robb, M. A.; Cheeseman, J. R.; Scalmani, G.; Barone, V.; Mennucci, B.; Petersson, G. A.; Nakatsuji, H.; Caricato, M.; Li, X.; Hratchian, H. P.; Izmaylov, A. F.; Bloino, J.; Zheng, G.; Sonnenberg, J. L.; Hada, M.; Ehara, M.; Toyota, K.; Fukuda, R.; Hasegawa, J.; Ishida, M.; Nakajima, T.; Honda, Y.; Kitao, O.; Nakai, H.; Vreven, T.; Montgomery Jr., J. A.; Peralta, J. E.; Ogliaro, F.; Bearpark, M.; Heyd, J. J.; Brothers, E.; Kudin, K. N.; Staroverov, V. N.; Kobayashi, R.; Normand, J.; Raghavachari, K.; Rendell, A.; Burant, J. C.; Iyengar, S. S.; Tomasi, J.; Cossi, M.; Rega, N.; Millam, J. M.; Klene, M.; Knox, J. E.; Cross, J. B.; Bakken, V.; Adamo, C.; Jaramillo, J.; Gomperts, R.; Stratmann, R. E.; Yazyev, O.; Austin, A. J.; Cammi, R.; Pomelli, C.; Ochterski, J. W.; Martin, R. L.; Morokuma, K.; Zakrzewski, V. G.; Voth, G. A.; Salvador, P.; Dannenberg, J. J.; Dapprich, S.; Daniels, A. D.; Farkas, Ö.; Foresman, J. B.; Ortiz, J. V.; Cioslowski, J.; Fox, D. J.; *Gaussian 09*, Revision B.01. Gaussian Inc., Wallingford, CT, USA, 2009.
30. Huang, W.; Manglik, A.; Venkatakrishnan, A. J.; Laeremans, T.; Feinberg, E. N.; Sanborn, A. L.; Kato, H. E.; Livingston, K. E.; Thorsen, T. S.; Kling, R. C.; Granier, S.; Gmeiner, P.; Husbands, S. M.; Traynor, J. R.; Weis, W. I.; Steyaert, J.; Dror, R. O.; Kobilka, B. K.; *Nature* **2015**, *524*, 315. [Crossref]
31. Dassault Systèmes, *Biovia Discovery Studio Visualizer*, v. 19; Dassault Systèmes, San Diego, CA, USA, 2018.
32. DeLano, W.; *PyMOL*, Schrödinger, Inc: New York, NY, USA, 2020. [Link] accessed in April 2023
33. Molander, G. A.; Cadoret, F.; *Tetrahedron Lett.* **2011**, *52*, 2199. [Crossref]
34. Chen, Y.-Y.; Chen, K.-L.; Tyan, Y.-C.; Liang, C.-F.; Lin, P.-C.; *Tetrahedron* **2015**, *71*, 6210. [Crossref]
35. Valdez, C. A.; Leif, R. N.; Mayer, B. P.; *PLoS One* **2014**, *9*, e108250. [Crossref]
36. Lipiński, P. F. J.; Szucs, E.; Jarończyk, M.; Kosson, P.; Benyhe, S.; Misicka, A.; Dobrowolski, J. C.; Sadlej, J.; *MedChemComm* **2019**, *10*, 1187. [Crossref]
37. Martin, Y. C.; *J. Med. Chem.* **2005**, *48*, 3164. [Crossref]
38. Brenk, R.; Schipani, A.; James, D.; Krasowski, A.; Gilbert, I. H.; Frearson, J.; Wyatt, P. G.; *ChemMedChem* **2008**, *3*, 435. [Crossref]
39. Baell, J. B.; Holloway, G. A.; *J. Med. Chem.* **2010**, *53*, 2719. [Crossref]
40. Li, J. G.; Chen, C.; Yin, J.; Rice, K.; Zhang, Y.; Matecka, D.; De Riel, J. K.; DesJarlais, R. L.; Liu-Chen, L. Y.; *Life Sci.* **1999**, *65*, 175. [Crossref]
41. Manglik, A.; Kruse, A. C.; Kobilka, T. S.; Thian, F. S.; Mathiesen, J. M.; Sunahara, R. K.; Pardo, L.; Weis, W. I.; Kobilka, B. K.; Granier, S.; *Nature* **2012**, *485*, 321. [Crossref]
42. Koehl, A.; Hu, H.; Maeda, S.; Zhang, Y.; Qu, Q.; Paggi, J. M.; Latorraca, N. R.; Hilger, D.; Dawson, R.; Matile, H.; Schertler, G. F. X.; Granier, S.; Weis, W. I.; Dror, R. O.; Manglik, A.; Skiniotis, G.; Kobilka, B. K.; *Nature* **2018**, *558*, 547. [Crossref]
43. Ricarte, A.; Dalton, J. A. R.; Giraldo, J.; *J. Chem. Inf. Model.* **2021**, *61*, 1251. [Crossref]
44. Schmidt, H. R.; Zheng, S.; Gurpınar, E.; Koehl, A.; Manglik, A.; Kruse, A. C.; *Nature* **2016**, *532*, 527. [Crossref]
45. Levoın, N.; Murthy, A. V. R.; Narendar, V.; Kumar, N. S.; Aparna, P.; Bhavani, A. K. D.; Reddy, C. R.; Mosset, P.; Grée, R.; *Bioorg. Med. Chem.* **2022**, *69*, 116851. [Crossref]
46. Díaz, J. L.; Cuevas, F.; Oliva, A. I.; Font, D.; Sarmentero, M. Á.; Álvarez-Bercedo, P.; López-Valbuena, J. M.; Pericàs, M. A.; Enrech, R.; Montero, A.; Yeste, S.; Vidal-Torres, A.; Álvarez, I.; Pérez, P.; Cendán, C. M.; Cobos, E. J.; Vela, J. M.; Almansa, C.; *J. Med. Chem.* **2021**, *64*, 5157. [Crossref]
47. Lipiński, P. F. J.; Matalińska, J.; *Int. J. Mol. Sci.* **2022**, *23*, 2766. [Crossref]
48. Szczepańska, K.; Podlewska, S.; Dichiarà, M.; Gentile, D.; Patamia, V.; Rosier, N.; Mönnich, D.; Ruiz Cantero, M. C.; Karcz, T.; Łażewska, D.; Siwek, A.; Pockes, S.; Cobos, E. J.; Marrazzo, A.; Stark, H.; Rescifina, A.; Bojarski, A. J.; Amata, E.; Kieć-Kononowicz, K.; *ACS Chem. Neurosci.* **2022**, *13*, 1. [Crossref]
49. Amata, E.; Dichiarà, M.; Gentile, D.; Marrazzo, A.; Turnaturi, R.; Arena, E.; la Mantia, A.; Tomasello, B. R.; Acquaviva, R.; Di Giacomo, C.; Rescifina, A.; Prezzavento, O.; *ACS Med. Chem. Lett.* **2020**, *78*, 889. [Crossref]
50. Zhuang, T.; Xiong, J.; Ren, X.; Liang, L.; Qi, Z.; Zhang, S.; Du, W.; Chen, Y.; Liu, X.; Zhang, G.; *Eur. J. Med. Chem.* **2022**, *241*, 114649. [Crossref]

Submitted: March 23, 2023

Published online: April 25, 2023

